ACS OMEGA

Article

http://pubs.acs.org/journal/acsodf

Deviation from van't Hoff Behavior of Solids at Low Temperature

Jan H. Sluyters* and Margaretha Sluyters-Rehbach

Ornstein Laboratory, Condensed Matter and Interfaces (CMI), Utrecht University, Princetonplein 1, 3584 CC Utrecht, Netherlands

ABSTRACT: As a sequel to results obtained on the low-temperature behavior of liquids, a similar study is presented for solids. A molecule in a solid interacts with the other molecules of the crystal so that it is subjected to a specific multimolecular potential, kT_0. At temperature $T < T_0$, the molecules are localized, and at $T > T_0$, they can participate in processes like self-diffusion and evaporation. As a consequence, the van't Hoff equation is disobeyed at a low temperature and properties like vapor pressure, diffusion rate, or reactivity are zero below the specific temperature, T_0, which here can be interpreted as a temperature of thermal stability of the solid. To account for this view, the van't Hoff equation, represented by the green curve in the figure, is extended with a suitable pre-exponential factor, leading to the red curve. Three examples, taken from the literature, are analyzed to demonstrate its applicability. These examples are: the thermal dissociation of calcium carbonate, the sublimation equilibrium pressure of naphthalene, and that of ice. For some other solids, equilibria and dynamic properties, $X(T)$, are examined by means of extrapolations in the $X(T)$ versus T domain, showing the presence of an arrest temperature, which coincides, within experimental accuracy, with the T_0 value obtained from the corresponding vapor pressure. As with liquids, kT_0 is found to be proportional to the molecular pair potential.

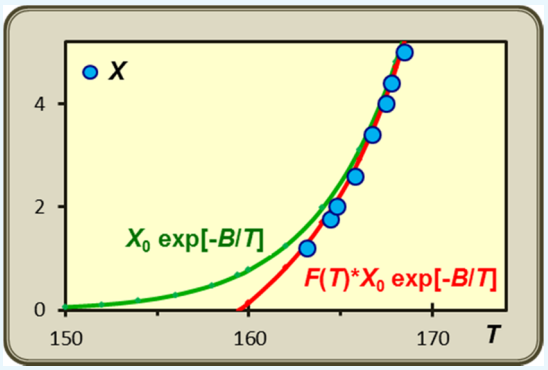

1. INTRODUCTION

> *"Although the great practical value of thermodynamics is undeniable, ..., there are certain limitations that must be borne in mind. The methods of thermodynamics are independent of atomic and molecular structure, and also of reaction mechanism." [Glasstone, Thermodynamics for Chemists, p. 1]*[1]

For a one-component object with two phases at equilibrium, the Phase Rule dictates that it can have only one degree of freedom.[2] This means that the choice of the value of one intensive property fixes the values of all other intensive properties. In the majority of cases, the temperature is the chosen property. Consequently, there must be an unequivocal relationship between any intensive property and temperature. The nature of such a relationship, that is, its mathematical form, however, remains undetermined and has to be derived from some other theory.

General agreement exists that thermodynamics is the theory that produces the expression for the temperature dependence of a property, X, and that it has an exponential form

$$X(T) = A \exp(-\Delta H/RT) \quad (1)$$

which is the integrated form of the van't Hoff equation. Its usual graphical representation is a plot of $\ln X(T)$ against $1/T$, known as the van't Hoff plot, which should be linear, so that its slope produces the enthalpy, ΔH, of an equilibrium.[2] This simple theory has met expectations in many fields in physics and physical chemistry and continues to be applied successfully, sometimes taking a weak temperature dependency of ΔH into account. (For its history, see, for instance, ref 3.) It has become common usage to describe the temperature dependence of the rate constants of the processes involved in the equilibrium with the Arrhenius equation, which takes the same form as eq 1, but with ΔH replaced by the heat of activation, $\Delta H^{\#}$.[2]

Equation 1 implies that $X(T)$ is zero at $T = 0$ K. However, in a series of three papers, we have collected substantial evidence that the (intensive) properties of liquids converge to zero at a finite temperature, T_0, which we named "arrest temperature".[4−6] In ref 4, primarily undertaken to investigate the electrical conduction by simple ions in water, we discovered that on extrapolation these conductivities all become zero at a finite temperature, $T_0 = 243$ K. Thereupon, we established that many more properties of water (e.g., self-diffusion, fluidity, vapor pressure) and of its solutes (e.g., diffusivity, solubility, reactivity) follow the same behavior.[5] The phenomenon was also shown to exist for a variety of other liquids, wherein, similarly, many properties converge to zero at the same finite temperature, T_0, a specific property of the liquid, always found to occur in its supercooled region.[6]

Considering this effect initially as a "property" of the (supercooled) liquid state, we gradually developed an understanding of it as an effective immobilization of the liquid owing to the increasing dominance of the molecular interactions in the system at lower temperatures.[6] Remarkably, T_0 was found to be proportional to the energy parameter ε/k of the molecular pair potential of the solvent.[6]

Received: February 13, 2017
Accepted: May 12, 2017
Published: May 25, 2017

DOI: 10.1021/acsomega.7b00169
ACS Omega 2017, 2, 2317−2325

It is the aim of this article to investigate whether such a temperature of arrest also occurs in the case of solids. This is important because the complicating metastability of a supercooled liquid is absent here. In contrast, for a solid, the arrest temperature, T_0, should, in principle, be directly experimentally accessible, and moreover, discussions on a so-called glassy or vitreous state will not apply. The meaning of this T_0 would be similar to the liquids' case, that is, a temperature below which the molecules in the solid are strictly immobilized.

As before,[4−6] our strategy was to collect literature data of experimental results on the temperature dependence of some property of a species and to extrapolate it toward a lower temperature. Because experimental results sometimes were reported after being corrected somehow, for these graphical analyses raw, unprocessed, experimental data will be used by preference. It should be remembered that such data were not measured with the intent to study the low-temperature behavior in particular but only to test the validity of eq 1. Generally, with modern techniques, extension of the studied temperature interval down to $T = T_0$, and also even below, may be possible for solids and with better accuracy.

However, besides equilibrium vapor pressure data, generally data on properties of a different kind are scarce for solids, and in many cases, one is limited to the vapor pressure, P, of a solid. Usually, P obeys van't Hoff's equation at a relatively high temperature, in conformity with eq 1. Deviation, leading to the observation of a T_0, requires some mathematical remodeling, which we will discuss in the next section. The applicability of these approaches will be investigated in detail for the CO_2 dissociation pressure of $CaCO_3$ and the vapor pressure of solid naphthalene and ice. Several further examples will be presented to show the general occurrence of arrest temperatures, T_0, of solids.

2. THEORETICAL APPROACH

Of course, the two different temperature dependences, that is, the familiar exponential at a high temperature, in conformity with eq 1, and a polynomial relationship that occurs at a low temperature, near T_0, at which $X(T)$ drops to zero, cannot hold true simultaneously. Clearly, they are to be combined in such a way that the two behaviors dominate in their respective temperature ranges, that is, at a high temperature according to eq 1 and at a low temperature polynomial, with a smooth transition in between. This can be accomplished, for example, by extending eq 1 with a pre-exponential factor, $F(T)$, according to

$$X(T) = F(T)A \exp(-\Delta H/RT) \tag{2}$$

and tentatively specifying $F(T)$ as

$$F(T) = 1 - \exp[-a(T - T_0)] \tag{3}$$

which satisfies both requirements if $T \geq T_0$.

The pre-exponential factor, $F(T)$, should represent the temperature-dependent fraction of the molecules that have a kinetic energy exceeding kT_0 and that consequently are able to participate in the process or equilibrium under consideration. As has been shown earlier, T_0 is a specific property of the condensed phase and should be identical for the different properties, X. The latter need not be necessarily so for parameter a.

It might be considered to further specify this definition, assuming the existence of a kinetic energy distribution function, $f(E, T)$, for the molecules. Then, the pre-exponential factor, $F(T)$, can be written as

$$F(T) = \frac{\int_{kT_0}^{\infty} f(E)\,\mathrm{d}E}{\int_0^{\infty} f(E)\,\mathrm{d}E} = 1 - \frac{\int_0^{kT_0} f(E)\,\mathrm{d}E}{\int_0^{\infty} f(E)\,\mathrm{d}E} \tag{4}$$

the integrals in which are generally named cumulative distribution functions. However, the kinetic energy distribution function is only known for a Maxwell−Boltzmann gas, that is, a gas without interaction. Yet, such an approach might, as an approximation, be useful as a (partial) justification of our eq 2. The rather phenomenological eq 3, however, has as yet more practical use.

Simply extrapolating available data as a function of temperature proved to be essentially useful to obtain T_0 in our studies of the liquids.[4−6] However, it may occur that at low temperatures, $X(T)$ drops, seemingly asymptotically, to very low values, almost coinciding with the temperature axis in a considerable temperature interval. In such cases of a so-called "hidden intercept", it will be helpful to plot some well-chosen power, y $[0 < y < 1]$ of the quantity $X(T)$ versus T. Applications of this procedure, which were explained in detail in ref 5, will also be shown and discussed below.

3. RESULTS AND DISCUSSION

3.1. Thermal Dissociation of Calcium Carbonate. In the thermal dissociation equilibrium reaction $CaCO_3 \leftrightarrow CaO + CO_2$, the pressure P of the evolved CO_2 is the only temperature-dependent property. For the following analysis, it is essential to avail of data of high precision in an extended temperature range, especially toward the low-temperature end. Such data are available in a study in 1956 by Hill and Winter,[7] giving the equilibrium CO_2 pressure at temperatures between 449 and 904 °C. These authors concluded from their experimental data that the simple exponential eq 1 applies to their whole temperature range, in contradiction with the earlier literature [see references in ref 7], in which additional terms were considered necessary for a fit. In Table 1, we illustrate the stepwise procedure followed presently to analyze the data in the whole temperature range.

3.1.1. Extrapolation. In columns 1 and 2, the data of ref 7 are reproduced, with temperature T in K and pressure P in Pa. Columns 3 and 4 list the values of $P^{0.5}$ and $P^{0.3}$ in the lower temperature range, which are used to construct the plots in Figure 1. On extrapolation, these plots intersect the horizontal axis at T_0 = 620−640 K, which indicates the existence of a temperature of arrest, as was explained in section 6 of our earlier paper.[5] Figure 1 also exhibits some points of the original data, $P(T)$, and a curve of P_{calc} versus T, derived from the involuted plots. Together, these three curves demonstrate the importance of the involution procedure.

3.1.2. van't Hoff Fit. In the next step, assuming that at a sufficiently high temperature the $CaCO_3/CaO+CO_2$ system behaves in accordance with eq 1, P values in the range $1177 > T > 1076$ K are fitted to an exponential of $1/T$. In Figure 2 it is shown that the "ideal" exponential behavior is indeed obeyed, described by

$$P_{id} = 1.0656 \times 10^{12} \exp(-18990/T) \tag{5}$$

3.1.3. Evaluation of F(T). Next, eq 5 is used to calculate P_{id} for the full temperature range, as listed in Table 1, column 5. Comparing with the experimental P by calculating P/P_{id}, it is

DOI: 10.1021/acsomega.7b00169
ACS Omega 2017, 2, 2317−2325

Table 1. Equilibrium CO_2 Pressure of the Reaction $CaCO_3 \leftrightarrow CaO + CO_2$,[7] and the Successive Mathematical Operations Described in the Text

T (K)	P (Pa)	$P^{0.5}$ $(Pa)^{0.5}$	$P^{0.3}$ $(Pa)^{0.3}$	P_{id} (Pa)	P/P_{id}	$F(T)$
722	2.27	1.51	1.28	4.03	0.563	0.438
738	4.40	2.10	1.56	7.12	0.618	0.496
753	6.44	2.54	1.75	11.89	0.542	0.544
766	10.75	3.28	2.04	18.24	0.589	0.583
781	17.07	4.13	2.34	29.36	0.581	0.623
801	34.93	5.91	2.90	53.88	0.648	0.671
813	53.00	7.28	3.29	76.45	0.693	0.696
827	77.19	8.79	3.68	113.53	0.680	0.724
837	106.79	10.33	4.06	149.36	0.715	0.742
852	149.32	12.22	4.49	222.70	0.671	0.767
869	269.98	16.43	5.36	344.42	0.784	0.792
880	327.97	18.11	5.69	452.60	0.725	0.807
888	419.96	20.49	6.12	549.73	0.764	0.817
905	701.27	26.48	7.14	821.50	0.854	0.837
913	899.92	30.00	7.70	987.32	0.911	0.846
929	1262.56	35.53	8.52	1412.65	0.894	0.861
935	1362.55	36.91	8.72	1610.66	0.846	0.867
946	1794.51	42.36	9.47	2039.71	0.880	0.876
959	2259.81	47.54	10.14	2677.62	0.844	0.887
971	3079.74	55.50	11.13	3420.02	0.901	0.896
979	3871.67	62.22	11.92	4012.68	0.965	0.901
992	5.05×10^3			5.17×10^3	0.975	0.909
1010	7.17×10^3			7.28×10^3	0.986	0.927
1020	8.69×10^3			8.75×10^3	0.993	0.932
1040	1.25×10^4			1.25×10^4	1.000	0.941
1058	1.67×10^4			1.69×10^4	0.985	0.948
1076	2.25×10^4			2.31×10^4	0.974	0.954
1089	2.92×10^4			2.85×10^4	1.026	0.958
1095	2.93×10^4			3.13×10^4	0.936	0.960
1105	3.62×10^4			3.66×10^4	0.987	0.963
1123	4.87×10^4			4.83×10^4	1.010	0.967
1126	4.96×10^4			5.05×10^4	0.982	0.968
1137	6.09×10^4			5.94×10^4	1.025	0.970
1143	6.60×10^4			6.49×10^4	1.017	0.972
1149	6.92×10^4			7.08×10^4	0.977	0.973
1159	7.79×10^4			8.16×10^4	0.954	0.975
1171	9.23×10^4			9.65×10^4	0.956	0.977
1177	1.08×10^5			1.05×10^5	1.034	0.978

seen in column 6 that eq 2 is fairly well obeyed down to T = ca. 992 K. At a lower temperature, P/P_{id} gradually decreases to about 0.5 at 750 K. Thus, a gradual deviation from van't Hoff behavior is observed on going to a lower temperature.

It is clear that P/P_{id} should equal the pre-exponential factor, $F(T)$, introduced in eq 2 and tentatively described by $F(T) = [1 - \exp(-a(T - T_0))]$. Its validity can be tested by fitting the data in column 6 to this expression. We find that the best fit gives T_0 = 640 K and a = 0.0067 K^{-1}. Using these results and eq 3, theoretical values of $F(T)$ are calculated, listed in column 7 of Table 1, and represented in Figure 3, together with the experimental results of column 6. The agreement is satisfactory, although the data are somewhat scattered.

It can be concluded that the thermal dissociation of $CaCO_3$ is arrested at a temperature T_0 = 630 ± 10 K and the corresponding deviation from ideal, thermodynamical, behavior is fairly well described by eqs 2 and 3.

3.2. Vapor Pressure of Solid Naphthalene. The sublimation equilibrium of naphthalene, which is a solid

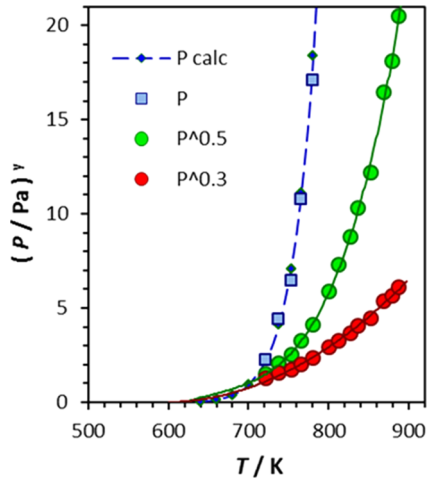

Figure 1. Construction of the arrest temperature of $CaCO_3$ by involution of the CO_2 equilibrium pressure[7] using two exponents. The plots comprise a temperature range of 500–900 K.

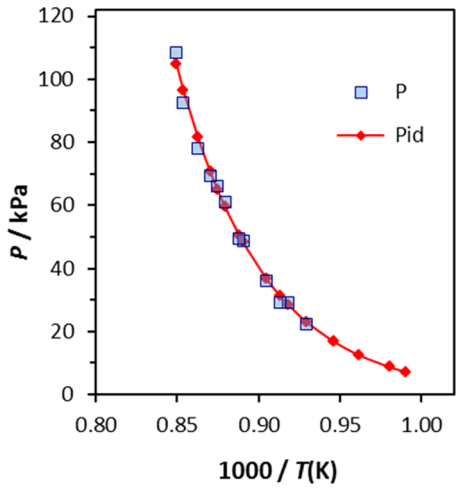

Figure 2. CO_2 vapor pressure of $CaCO_3$ in the high-temperature region, with P data in the range of 1177–1076 K. The red curve is calculated with eq 5 and extended to T = 1010 K.

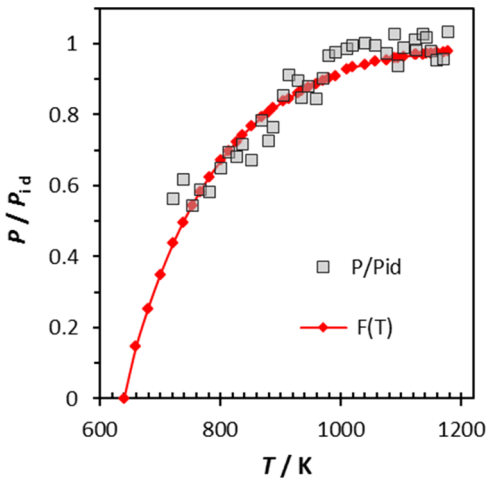

Figure 3. Deviation from van't Hoff behavior, expressed by P/P_{id}, as described in the text, depends on the temperature according to the proposed pre-exponential factor, $F(T) = 1 - \exp[-a(T - T_0)]$.

DOI: 10.1021/acsomega.7b00169
ACS Omega 2017, 2, 2317–2325

below 353.55 K, has been widely accepted as a model system for the calibration of devices measuring vapor pressures. Consequently, vapor pressures as a function of temperature have been accurately determined several times with very good agreement. For our purpose, we selected two reports[8,9] that include data at higher temperatures, that is, 253 < T < 353 K, and two reports[10,11] particularly focused at low temperatures, at about 240 < T < 260 K. Inevitably, the latter data are less precise. Nevertheless, Figure 4 shows that the results for $P^{0.5}$ versus T fit very well together.

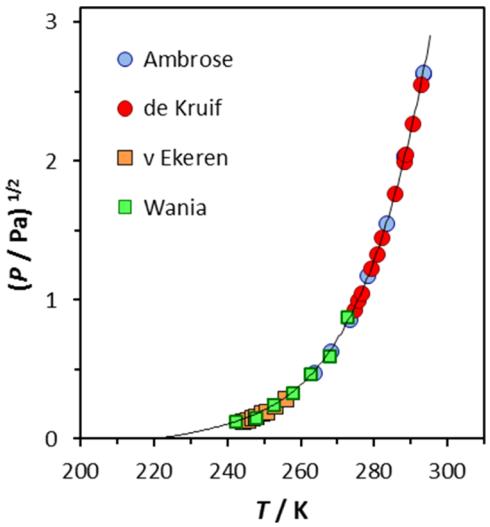

Figure 4. Square root of the vapor pressure of solid naphthalene, obtained from different authors,[8−11] as indicated, extrapolated to the arrest temperature.

The analysis, following the same route as described for $CaCO_3$, leads to the following results:

(i) The intersection of the plot in Figure 4 gives an arrest temperature, T_0 = 222 K.

(ii) The plot of P versus $1/T$ in the region 353 > T > 303 K is found to obey eq 1 with

$$P_{id} = 3.25 \times 10^{13} \exp(-8550/T) \quad (6)$$

(iii) The value of P/P_{id} is close to unity down to ca. 285 K and then decreases to become about 0.8 at 244 K. Naturally, it is zero at the arrest temperature, T_0 = 222 K. Numerical fit of these results to the expression in eq 3 for the pre-exponential factor produces the red curve in Figure 5 and a = 0.044 K^{-1}.

3.3. Vapor Pressure and Dielectric Relaxation of Ice.

An extensive literature exists on the vapor pressure and the heat of sublimation of ice. From a well-documented review by Murphy and Koop,[12] it follows that eq 1 applies adequately in the temperature region 175 < T < 273, whereas also more elaborate parameterizations have been proposed, for example, in the frequently cited theoretical work of Wexler.[13] We selected both the recently presented data of Bielska et al.[14] and the earlier study by Marti and Mauersberger[15] and found these to obey

$$P_{id} = 3.647 \times 10^{12} \exp(-6148.5/T) \quad (7)$$

in the above-mentioned region. Later, however, Mauersberger and Krankowsky[16] were able to extend the temperature range

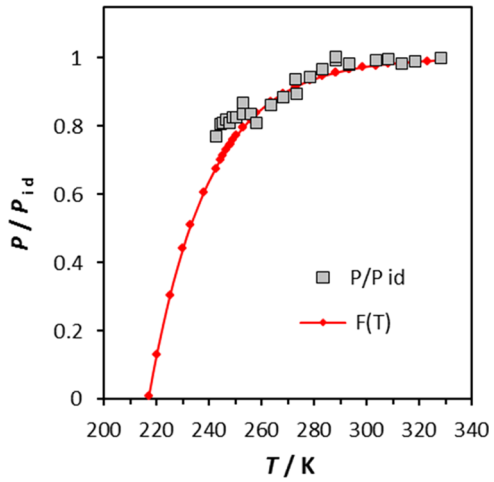

Figure 5. Experimental temperature dependence of the pre-exponential factor for solid naphthalene.

down to 164.5 K and thereby observed a significant departure from eq 7. Their data were displayed in a logarithmic graph, from which we obtained pressure values that are as accurate as possible. In Figure 6, it is shown that the combined data of refs 14 and 16 connect nicely into one continuous plot, which easily extrapolates to P = 0 at T_0 = ca. 160 K.

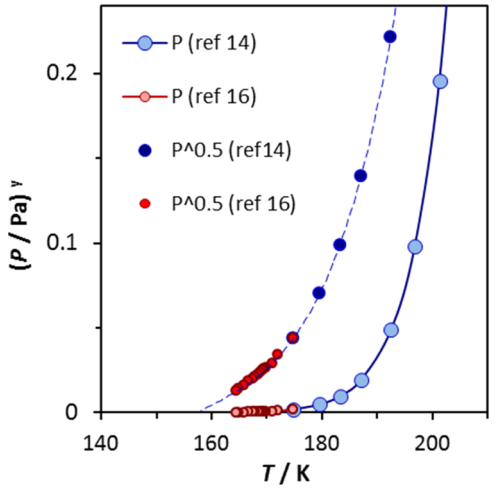

Figure 6. Experimental ice vapor pressure[14−16] arrests at 160 K. Both P and $P^{0.5}$ are plotted.

Following the analysis described in the foregoing sections, we find that P/P_{id} is close to unity from T = 273 K down to 169 K but decreases thereafter according to $P/P_{id} = [1 - \exp(-a(T - T_0))]$, with a = 0.45 K^{-1} and T_0 = 158 K. With this high value for a, the plot of P/P_{id} against T sharply bends toward the arrest temperature, as shown in Figure 7. Notably, the additional data of ref 16 are essentially valuable for the analysis.

Ice is an important substance and so besides vapor pressure several more of its properties have been described in the literature, which may support our value of T_0, although one would wish for more accurate data points at low temperatures. A possible example is the dielectric relaxation of ice-Ih as a function of temperature, which was the subject of the pioneering study in 1958 by Auty and Cole.[17] In later work by other researchers, severely different results were reported, which only recently could be ascribed to the manner of

DOI: 10.1021/acsomega.7b00169
ACS Omega 2017, 2, 2317−2325

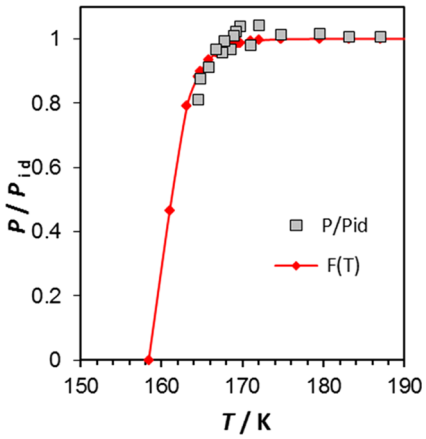

Figure 7. Pre-exponential factor for ice derived from analysis of the vapor pressure.

preparation of the ice specimen.[18] From the latter study, it follows that the data obtained by slow crystallization of the ice, as performed in ref 17, are to be preferred. A plot of the reciprocal of the dielectric relaxation time, τ, in Figure 8 produces T_0 = 170 K, close to the value of 160 K found from the vapor pressures.

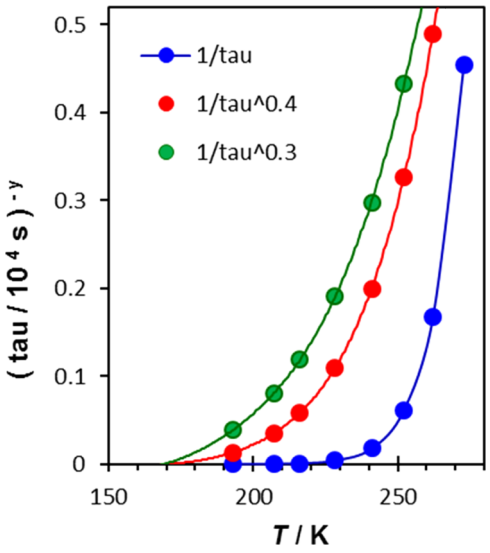

Figure 8. Reciprocal of the dielectric relaxation time of ice-Ih extrapolates to zero at 170 K.

The T_0 of ice, 160 K, is far below the T_0 of water, 243 K. This explains the puzzling intersection of the vapor pressure lines of ice and supercooled water against T, discussed by Kraus and Greer[19] and ourselves.[5] Also, it shows that the multimolecular potential, defined as kT_0,[6] of ice is 0.66 times its value for water. This agrees with the more open structure of ice, with its larger intermolecular distances, as follows from its low density. Further analysis produced a = 0.051 K^{-1} for liquid water, about 10 times smaller than that for ice.

3.4. Vapor Pressures of Pure Substances. In the three cases of low-temperature behavior reported above, significant deviation from eq 1 could be demonstrated. Also, it is clear that the parameters a and T_0 in eq 3 characterize the temperature range in which the deviation shows up. On the other hand, the extrapolations cover also the higher temperatures where van't Hoff behavior prevails at least apparently. This encourages the idea that the extrapolation approach, leading to the arrest temperature, is valid more generally, also when the low-temperature data are not available.

This happens to be the case with vapor pressures of pure substances available from the extensive collections of $P-T$ relations of both organic and inorganic compounds.[20] Here, we select three examples with relatively small molecules, CH_4, CO_2, and NH_3, plotted in Figure 9. The T_0 values are obtained

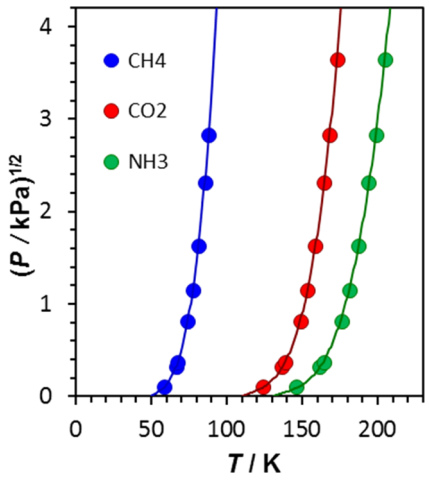

Figure 9. Square root of the vapor pressures of solid CH_4, CO_2, and NH_3[20] plotted against temperature shows the three T_0 's at 50, 110, and 130 K, respectively.

from extrapolations by eye and next drawing with polynomials of the appropriate degree. In the present case, $P^{1/2}$ is plotted, which provides a clear picture with a sharp intersection of the temperature axis.

3.5. Hydrates and Ammoniacates. The salt $Mg(ClO_4)_2$ easily associates with H_2O to form distinct solid hydrates with 2, 4, or 6 water molecules. Depending on the amount of water, at equilibrium, mixtures of only two of these salt hydrates will always occur. The water vapor pressure of a mixture then equals the pressure of the highest hydrate.

Besley and Bottomley[21] studied the equilibrium vapor pressures of the following mixtures:

A. $Mg(ClO_4)_2 \cdot 6aq + Mg(ClO_4)_2 \cdot 4aq$
B. $Mg(ClO_4)_2 \cdot 4aq + Mg(ClO_4)_2 \cdot 2aq$
C. $Mg(ClO_4)_2 \cdot 2aq + Mg(ClO_4)_2$

With two components, $Mg(ClO_4)_2$ and H_2O, and three phases (two hydrates and the vapor), one degree of freedom remains,[2] that is, a single $P-T$ relationship for each of the three pairs. Figure 10 shows the appurtenant equilibrium water vapor pressures as a function of temperature. The three curves appear to coincide in a common intersection point with the temperature axis, at T_0 = 240–250 K, which is remarkably close to the T_0 of pure supercooled water.[4,5]As at that temperature, 243 K, salts are insoluble in water,[4,5] the intersection might indicate a separation of the hydrates into water and dehydrated magnesium perchlorate. Probably also the vapor pressures of saturated $MgClO_4$ solutions against temperature will fit in Figure 10. Similar behavior occurs with the three ammoniacates of AgCl.[22]

3.6. Properties of Metals. From several studies, we obtained the temperature dependence of the self-diffusion of silver[23] and of gold[24] as well as the trace diffusion of silver in

DOI: 10.1021/acsomega.7b00169
ACS Omega 2017, 2, 2317–2325

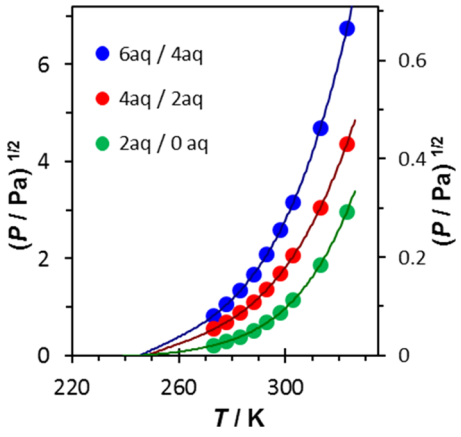

Figure 10. Square root of water vapor pressure plotted against temperature of the three pairs of magnesium perchlorate hydrates.[21] Left-hand axis: 6aq/4aq and 4aq/2aq; right-hand axis: 2aq/0aq.

(pure) gold and of gold in (pure) silver.[25] The data, represented in Figure 11, form a family of curves, all with

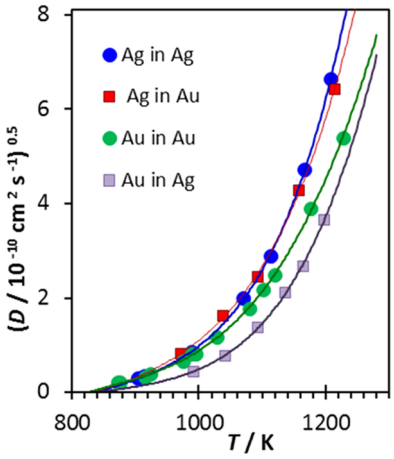

Figure 11. Self-diffusion and trace diffusion in gold and silver.[23−25] For explanation see text.

arrest temperature T_0 = 840 K. As can be expected, the two processes that occur in gold have the same T_0. Likewise, the self-diffusion of silver and the diffusion of gold in silver will become zero at an identical T_0 value. Remarkably, the T_0 's of the gold and silver systems are also very close. This may be considered to be accidental, possibly owing to the almost equal atomic radii of the two metals.

The vapor pressure[26] of solid polycrystalline zinc and self-diffusion coefficients[27] of single crystalline zinc all extrapolate to zero at T_0 = 510 K, as shown in Figure 12.

3.7. Mobility of Vacancies in Doped Crystals. The electrical conductance of solid alkali halides proceeds mainly by the motion of cation vacancies present in the "pure" crystal, and is increased by doping the crystal with divalent cations. In Figure 13 are shown the conductivity data for single crystalline NaCl doped with $CdCl_2$, measured by Etzel and Maurer[28] and tabulated by Lidiard.[29]

It is commonly assumed that in a certain temperature region the conductivity, σ, should obey a relationship of the type $\sigma = (A/T) \exp[-B/T]$. In ref 28, this is indeed observed for 520 < T < 680 K. However, the plots in Figure 13 fit nicely to a family of curves converging to a common intersection point at T_0 =

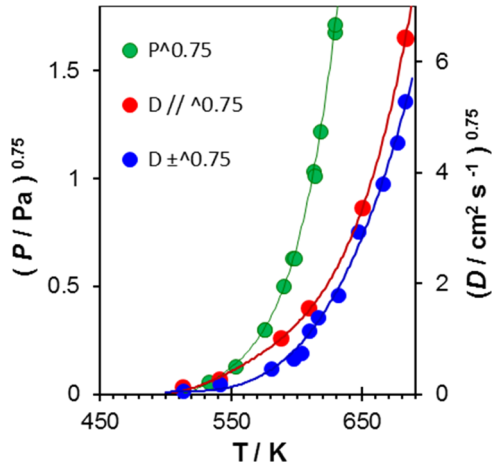

Figure 12. Vapor pressure of polycrystalline zinc[26] and self-diffusion coefficients of single-crystalline zinc[27] arrest at the same temperature. $D//$ and $D\pm$ indicate the diffusivities parallel and perpendicular to the symmetry axis, respectively.

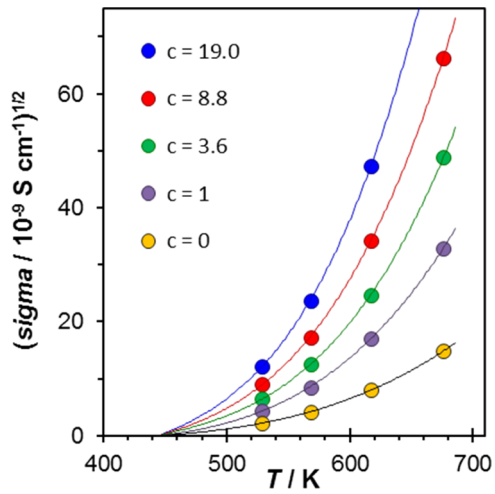

Figure 13. Square root of electrical conductivity of sodium chloride,[28,29] doped with $CdCl_2$ in varied concentrations, producing the same T_0. The mole fraction of $CdCl_2$ is equal to $10^{-5}c$.

450 K, which obviously can be considered to be the arrest temperature of solid sodium chloride.

3.8. Solubility of Hydrogen in Metals. A property of hydrogen is its capacity to dissolve in several metals in the form of atomic H. In transition metals like nickel, cobalt, rhodium, and so on, the solubility decreases with decreasing temperature.[30] In Figure 14, this is shown for polycrystalline nickel and rhodium as the solvents, with T_0 values of 380 and 750 K, respectively. A similar plot for cobalt,[31] the properties of which are close to those of nickel, has an arrest temperature of 520 K. However, in single crystalline nickel,[31] the solubility is much lower, and T_0 = 570 K.

3.9. Vapor Pressures of Solid Noble Gases. In our previous paper,[6] it was shown that for the noble gases in the (supercooled) liquid state, an arrest temperature is obtained on plotting the equilibrium vapor pressure, the fluidity, or the diffusivity versus temperature. Vapor (sublimation) pressures of solidified noble gases are also available, and have been collected by Pollack with the purpose of testing the applicability of the law of corresponding states.[32] With the exception of neon, the corresponding states law was found to apply.[32,33] In Figure 15,

DOI: 10.1021/acsomega.7b00169
ACS Omega 2017, 2, 2317−2325

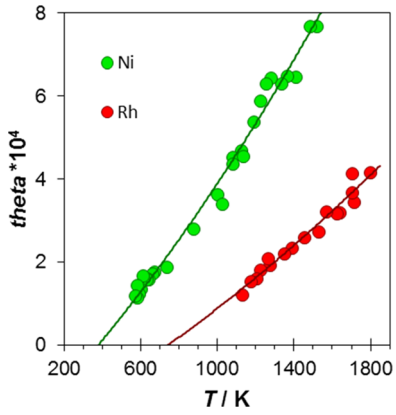

Figure 14. Solubility of hydrogen in nickel and in rhodium,[30] expressed by its mole fraction, ϑ, as a function of temperature.

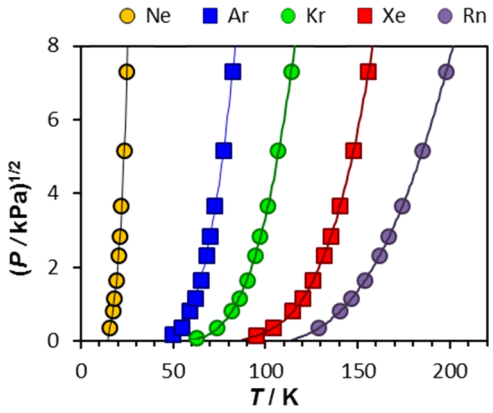

Figure 15. Vapor pressures of solid noble gases[20,33] are zero at their respective T_0's.

we use the large data set of Leming and Pollack[33] for solid argon, krypton, and xenon, and the data collected in ref 20 for solid neon and radon. The resulting arrest temperatures are 13, 45, 58, 88, and 115 K respectively.

These T_0 values might obey a corresponding state relationship as well. We choose to test this by calculating the reduced arrest temperature, $T_{0,r} = T_0/T_c$, where T_c is the critical temperature. The result is 0.29, 0.30, 0.285, 0.30, and 0.305, for Ne, Ar, Kr, Xe, and Rn, respectively.

4. RELATION BETWEEN T_0 AND MOLECULAR PAIR POTENTIAL

In our earlier paper concerning the behavior of liquids,[6] we discussed extensively the possibility of a linear relationship between the arrest temperature and the parameter ε/k, which is an essential quantity in, for example, the Lennard-Jones or the Stockmayer formulation of the pair potential between simple spherical or quasispherical molecules. Indeed, for a considerably broad selection of such molecules, this linearity could be established.

Table 2 gives a selection of simple molecules for which we have evaluated the T_0 values of the solid phase and for which ε/k values are available from the literature.[34−36] The arrest temperatures are tabulated both for the liquid and the solid phases. In Figure 16, these T_0's are plotted versus ε/k showing that, indeed, a linear relationship appears to hold also for the solid phase.

Table 2. Compilation of the Energy Parameter, ε/k, and Arrest Temperature, T_0, of the Liquid and Solid, expressed in K, for a Selection of Simple Molecules[a]

species	ε/k	T_0 liquid	T_0 solid
Ne	32	17	10
CO	105	40	40
Ar	112	55	45
CH_4	140.4	58	50
Kr	155	72	55
Xe	214	94.5	75
N_2O	248.8	120	102
Rn	280		115
Cl_2	296	140	
NH_3	310	155	130
H_2O	450	242	150

[a]See text.

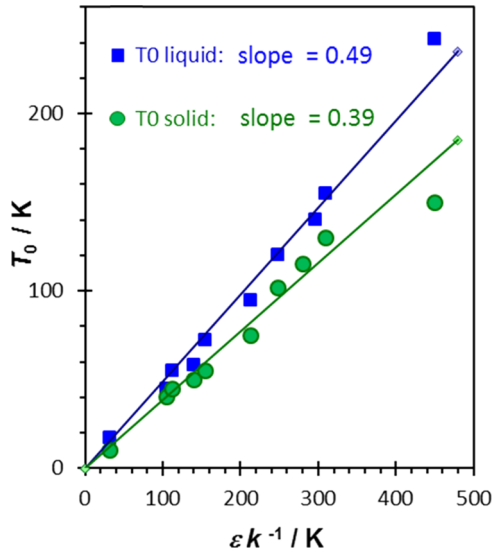

Figure 16. Linear relationship between the arrest temperatures of liquids and solids and the energy parameter in the Lennard-Jones or Stockmayer pair potential, using the data from Table 2.

In ref 6, we proposed to define the multimolecular potential, kT_0, as the Boltzmann energy, below which the mutual interactions of the molecules keep them locally stuck. The stronger the interaction, the higher the temperature at which, for instance, evaporation or (self)diffusion starts. From the slopes of the lines in Figure 16, it follows that the multimolecular potential of a solid is about 0.8 times that of the corresponding supercooled liquid.

5. CONCLUSIONS

At the end of the 19th century, after the van't Hoff equation for the quantitative description of the temperature dependence of chemical and physical equilibria was introduced, it became general practice to report logarithms of experimental equilibrium and rate constants, plotted versus $1/T$. Also the more recent, sometimes complex, theoretical calculations on reaction rates invariably contained a term like $\exp[-B/T]$ as the dominating part,[37,38] and prompted similar logarithmic representations.

However, taking a logarithm is apt to reduce the resolution of data and obscure a possible deviation from the accepted model. After having discovered the deviant low-temperature behavior

DOI: 10.1021/acsomega.7b00169
ACS Omega 2017, 2, 2317−2325

in the case of water[4,5] and other liquids,[6] we believe that the direct extrapolation of data versus T toward lower temperature is to be preferred, if necessary, after involution[5,6] of the experimental data. The latter must be done with care, applying several values of the power y mentioned in Section 2.

In addition, in the present article, we propose an extension of the van't Hoff equation, eq 2, with the tentative formulation of $F(T)$ in eq 3. We note that the latter expression is mathematically the simplest conceivable. From the three examples in Figures 3, 5, and 7, it can be deduced that the "steepness parameter" a can attain strongly variant values, thus determining the temperature range in which the decline toward the arrest takes place. These three examples provide strong evidence that the direct extrapolations really lead to a temperature, T_0, where the pressure becomes zero. The examples involving rates (diffusion in metals, conductance in doped crystals) or solubilities (hydrogen in metals) corroborate this view.

To our knowledge, the possibility of a breakdown of the van't Hoff behavior owing to the increasing domination of molecular interactions at low temperature has not been recognized earlier for cases involving solids. In contrast, it is generally believed that vapor pressures, although very low, remain finite down to 0 K.

The several examples presented here may initiate more investigations of the same type. To this end, the range and accuracy of data reported in the literature could be improved with present-day techniques. The obtained arrest temperatures, then, could be compared with the molecular pair potential to further confirm the interesting proportionality shown in Figure 16.

AUTHOR INFORMATION

Corresponding Author

*E-mail: sluyters@freeler.nl.

ORCID

Jan H. Sluyters: 0000-0002-7122-3880

Notes

The authors declare no competing financial interest.

REFERENCES

(1) Glasstone, S. *Thermodynamics for Chemists*; Van Nostrand Company: New York, 1947; p 1.

(2) Glasstone, S. *Elements of Physical Chemistry*; Van Nostrand Company: New York, 1946; pp 195−200, 316−320.

(3) Laidler, K. J. *The World of Physical Chemistry*; Oxford University Press: Oxford, 1951; pp 238−242.

(4) Sluyters, J. H.; Sluyters-Rehbach, M. Rotation of Water Molecules and its Relation with the Chemistry and Physics of Liquid Water. *J. Phys. Chem. B* **2010**, *114*, 863−869.

(5) Sluyters, J. H.; Sluyters-Rehbach, M. Temperature Dependence of the Properties of Water and its Solutes, Including the Supercooled Region. *ChemPhysChem* **2013**, *14*, 3788−3800.

(6) Sluyters, J. H.; Sluyters-Rehbach, M. Arrest as a General Property of the Supercooled Liquid State. *J. Phys. Chem. B* **2016**, *120*, 3735−3745.

(7) Hill, K. J.; Winter, E. R. S. Thermal Dissociation Pressure of Calcium Carbonate. *J. Phys. Chem.* **1956**, *60*, 1361−1362.

(8) Ambrose, D.; Lawrenson, I. J.; Sprake, C. H. S. The vapor Pressure of Naphthalene. *J. Chem. Thermodyn.* **1975**, *7*, 1173−1175.

(9) De Kruif, C. G.; Kuipers, T.; van Miltenburg, J. C.; Schaake, R. C. F.; Stevens, G. The vapor Pressure of Solid and Liquid Naphthalene. *J. Chem. Thermodyn.* **1981**, *13*, 1081−1086.

(10) Van Ekeren, P. J.; Jacobs, M. H. G.; Offringa, J. C. A.; de Kruif, C. G. *J. Chem. Thermodyn.* **1983**, *15*, 409−417.

(11) Wania, F.; Shiu, W. Y.; Mackay, D. Measurement of the Vapor Pressure of Several Low-Volatility Organochlorine Chemicals at Low Temperatures with a Gas Saturation Method. *J. Chem. Eng. Data* **1994**, *39*, 572−577.

(12) Murphy, D. M.; Koop, T. Review of the vapor Pressures of Ice and Supercooled Water for Atmospheric Applications. *Q. J. R. Meteorol. Soc.* **2005**, *131*, 1539−1565.

(13) Wexler, A. Vapor Pressure Formulation for Ice. *J. Res. Natl. Bur. Stand., Sect. A* **1977**, *81A*, 5−20.

(14) Bielska, K.; Havey, D. K.; Scace, G. E.; Lisak, D.; Harvey, A. H.; Hodges, J. T. High-Accuracy Measurements of the Vapor Pressure of Ice Referenced to the Triple Point. *Geophys. Res. Lett.* **2013**, *40*, 6303−6307.

(15) Marti, J.; Mauersberger, K. A. Survey and New measurements of Ice Vapor Pressure at Temperatures Between 170 and 250 K. *Geophys. Res. Lett.* **1993**, *20*, 363−366.

(16) Mauersberger, K.; Krankowski, D. Vapor Pressure above Ice at Temperatures Below 170 K. *Geophys. Res. Lett.* **2003**, *30*, 1121−1123.

(17) Auty, P.; Cole, R. H. Dielectric Relaxation of Ice and Solid D_2O. *J. Chem. Phys.* **1952**, *20*, 1309−1314.

(18) Sasaki, K.; Kito, R.; Shinyashiki, N.; Yagihara, S. Dielectric Relaxation Time of Ice-Ih with Different Preparation. *J. Phys. Chem. B* **2016**, *120*, 3950−3953.

(19) Kraus, G. F.; Greer, S. C. Vapor Pressures of Supercooled H_2O and D_2O. *J. Phys. Chem.* **1984**, *88*, 4781−4785.

(20) Stull, D. R. Vapor Pressure of Pure Substances, (a) Organic Compounds, (b) Inorganic Compounds. *Ind. Eng. Chem.* **1947**, *39*, 517−550.

(21) Besley, L. M.; Bottomley, G. A. The Water vapor Equilibria over Magnesium Perchlorate Hydrates. *J. Chem. Thermodyn.* **1969**, *1*, 13−19.

(22) Findlay, A.; Campbell, A. N.; Smith, N. O. *The Phase Rule and Its Applications*, 9th ed.; Dover Publications: New York, 1951; p 217.

(23) Tomizuka, C. T.; Sonder, E. Self-Diffusion in Silver. *Phys. Rev.* **1956**, *103*, 1182−1184.

(24) Okkerse, B. Self-diffusion of Gold. *Phys. Rev.* **1956**, *103*, 1246−1249.

(25) Mallard, W. C.; Gardner, A. B.; Bass, R. F.; Slifkin, L. M. Self-Diffusion in Silver-Gold Solid Solutions. *Phys. Rev.* **1963**, *129*, 617−625.

(26) Coleman, F. F.; Egerton, A. A Study of the vapor Pressures of Magnesium, Thallium and Zinc, and the Determination of their Chemical Constants. *Philos. Trans. R. Soc., A* **1935**, *234*, 177−204.

(27) Shirn, G. A.; Wajda, E. S.; Huntington, H. B. Self-diffusion in Zinc. *Acta Metall.* **1953**, *1*, 513−518.

(28) Etzel, H. W.; Maurer, R. J. The Concentration and Mobility of Vacancies in Sodium Chloride. *J. Chem. Phys.* **1950**, *18*, 1003−1007.

(29) Lidiard, A. B. Ionic Conductivity of Impure Polar Crystals. *Phys. Rev.* **1954**, *94*, 29−37.

(30) McLellan, R. B.; Oates, W. A. The Solubility of Hydrogen in Rhodium, Ruthenium, Irridium and Nickel. *Acta Metall.* **1973**, *21*, 181−185.

(31) Stafford, S. W.; McLellan, R. B. The Solubility of Hydrogen in Nickel and Cobalt. *Acta Metall.* **1974**, *22*, 1463−1468.

(32) Pollack, G. L. Extension of the Law of Corresponding States to Rare-Gas Solids. *Phys. Rev. A* **1970**, *2*, 38−42.

(33) Leming, C. W.; Pollack, G. L. Sublimation Pressures of Solid Ar, Kr, and Xe. *Phys. Rev. B* **1970**, *2*, 3323−3330.

(34) Mourits, F. M.; Rummens, F. H. A. A Critical Evaluation of Lennard-Jones and Stockmayer potential Parameters and of some Correlation Methods. *Can. J. Chem.* **1977**, *55*, 3007−3020.

(35) Cuadros, F.; Mulero, A.; Cachadina, J.; et al. A New Procedure for Determining Lennard-Jones Interaction Parameters. *Int. Rev. Phys. Chem.* **1995**, *14*, 205−213.

(36) Cuadros, F.; Cachadina, J.; Ahumada, W. Determination of Lennard-Jones interaction Parameters using a new Procedure. *Mol. Eng.* **1996**, *6*, 319−325.

DOI: 10.1021/acsomega.7b00169
ACS Omega 2017, 2, 2317−2325

(37) See for instance: Glasstone, S.; Laidler, K. J.; Eyring, H. *The Theory of Rate Processes*; McGraw-Hill: New York, 1941; Chapter 1.
(38) Truhlar, D. G.; Hase, W. L.; Hynes, J. T. Current Status of Transition State Theory. *J. Phys. Chem.* **1983**, *87*, 2664−2682.

DOI: 10.1021/acsomega.7b00169
ACS Omega 2017, 2, 2317−2325